IEEE Access
Multidisciplinary | Rapid Review | Open Access Journal

IEEE POWER & ENERGY SOCIETY SECTION

Received March 31, 2021, accepted April 20, 2021, date of publication April 26, 2021, date of current version May 10, 2021.

Digital Object Identifier 10.1109/ACCESS.2021.3075463

Evaluation Scheme of Voltage Sag Immunity in Sensitive Industrial Process

ANJUNGUO HUANG, XIANYONG XIAO, (Senior Member, IEEE), AND YING WANG, (Senior Member, IEEE)
College of Electrical Engineering, Sichuan University, Chengdu 610065, China

Corresponding author: Xianyong Xiao (1269962362@qq.com)

This work was supported by the Project of the National Natural Science Foundation of China under Grant 51807126.

ABSTRACT In order to enhance the effectiveness of voltage sag governance and the practicability of the process immunity assessment method, an immunity assessment method for the assembly line process is proposed, fully considering the relationship between logistics line and power line, and thoroughly portraying the relationship between equipment and its links in depth. Combined with the existing voltage tolerance curve test results, the power line immunity time is reasonably evaluated considering the response delay of each device. In addition, the fault probability is quantified considering the possibility of equipment failure and its link repairing. On this basis, the minimal cut-set method is adapted to standardize the constructed random network of logistics lines. The immunity of the whole manufacturing process is evaluated through series-parallel logical analysis. In the end, the paper mill is taken as a sample to illustrate the proposed method. The deviation between the average annual economic loss obtained from model evaluation and this typical producer's survey loss is regarded as the basis for the measurement of the effectiveness of the method. The results show that the immunity of the process can be accurately evaluated for the deviation of the evaluation obtained by the proposed method is relatively small.

INDEX TERMS Voltage sag, voltage tolerance curve, process immunity time, minimal cut set.

I. INTRODUCTION

During the sensitive industrial process, there are numerous control and motor driving equipment that are sensitive to voltage sag and power supply interruption. Equipment failure caused by a voltage sag or interruption event will often lead to disruption of production and serious comprehensive economic losses [1]–[5]. The development of loss assessment and the design of the treatment scheme is based on the effective assessment of voltage sag and interruption immunity during the process of production. Therefore, it is necessary to make research on the method of voltage sag and interruption immunity assessment for sensitive industrial processes.

The evaluation of fault probability on voltage sag of sensitive equipment is usually based on the voltage tolerance curve (VTC) model of equipment. A large number of existing studies have tested the VTC of various sensitive equipment. Literature [6]–[8] test different types of AC contactors (ACC), and summarized the shape of VTC. Literature [9] analyzes the influence of temporary voltage sag value, duration, phasor type, and different load conditions on voltage sag immunity of Adjustable Speed Drive (ASD) by comparing the test results of VTC. Literature [10] discusses the VTC test results of several personal computers (PC).

The key to process immunity assessment is to construct a logical relationship model among equipment so as to estimate the overall process fault probability based on the equipment failure probability. Some scholars have studied the boundary parameters and logical relationship structure of VTC, which can be adjusted adaptively according to the sample data [11]. Literature [12] proposes a three-level risk assessment model, which includes equipment, sub-process, and process, from the voltage sag or interruption to production failure. It also evaluates the process immunity with fault tree analysis. Literature [13] analyzes varieties of typical sensitive equipment, constructs immunity time index based on producing process parameters, and puts forward a general idea of process evaluation from the perspective of process parameters. Literature [14] introduces the series-parallel model to describe the logical relationship between equipment and process. On the basis of the previous study, the author considers the influence of the action characteristics of protection mechanisms such as

The associate editor coordinating the review of this manuscript and approving it for publication was Suman Maiti.

reclosing on the evaluation of outage probability again, and makes a special study on the influence of short-term power supply interruption caused by reclosing [15], [16]. Literature [14] considers how to combine the process immunity time with a single typical sensitive device in the link, but it does not Considering that multiple sensitive devices with electrical connections in the link constitute the power line structure, it is not explained how to coordinate the immune time of multiple sensitive modules such as ASD and motors. Literature [17] conducted a test study on the sag tolerance of the link composed of the typical power line structure of ACC-ASD-motor, but did not consider how to evaluate the sag immunity of the entire industrial process composed of different links. Literature [11], [18] considers different types of sensitivity in the unified link how to evaluate the failure probability of the combination of equipment, and also consider the industrial process logistics line composed of different links, but this method does not give the evaluation and calculation method of process immunity time (PIT).

Therefore, it is also necessary to determine how to determine the different sensitivity in each link. The power line composed of equipment is combined with the logistics line composed of different links, and on this basis, a reasonable PIT evaluation calculation method is given for further research. The main contributions of this thesis are as follows:

(1) This thesis proposes a general industrial process structure to describe the relationship between the power line of power transmission and the logistics line of product transmission. The typical sensitive industrial power structure composed of ACC, ASD, and motors is unified with the traditional logistics line structure (industrial process structure) of each link analyzed by the series-parallel module method and the fault tree method. It further clarified how to consider the concept of PIT in the evaluation of process immunity.

(2) This thesis also proposes a PIT evaluation method for the ASD-motor sag-sensitive structure widely existing in the industrial process, and gives a convenient calculation formula.

(3) This thesis uses the minimum cut set method to convert the module diagram that is consistent with the pipeline structure and is easy to draw but the logical relationship is not clear into a standardized module connection diagram with a clear serial and parallel logic relationship. It is more conducive for researchers to obtain probability expressions based on the evaluation knowledge of component-system reliability in the basic probability theory, so as to solve the failure probability relationship between each link and process.

II. RELATED CONCEPTS

A. PROCESS IMMUNITY TIME

PIT is defined as the time from the moment of voltage sag to the time when the process parameters of the studied process exceed the threshold and thus be judged as failure [14], which here in after refers to as immunity time, as shown in Fig. 1.

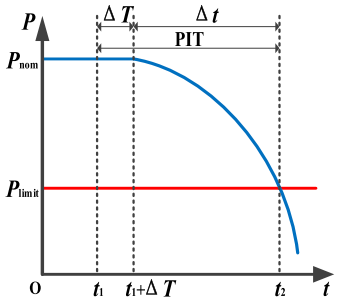

FIGURE 1. Schematic diagram of process immunization time.

In Fig.1, P_{nom} is rated parameters value, P_{limit} is threshold. t_1 and t_2 represent the time when sag occurs and when the parameters exceed the threshold. ΔT is the response dead time and Δt is the fault response time of the sensitive equipment.

B. VOLTAGE TOLERANCE CURVE AND VOLTAGE-IMMUNITY TIME CURVE

VTC is mainly used to describe the two basic characteristics of voltage sag, namely amplitude and duration. The points on the curve are composed of critical voltage sag events that lead to the failure of sensitive equipment. An event on the lower right side of the curve causes the device to fail. As shown in Fig. 2, the duration of the critical voltage sag event in the region where the VTC amplitude is lower than the horizontal segment of the curve is defined, in this thesis, as the critical duration (CD) of the equipment. When the duration of the sag exceeds CD at the corresponding amplitude, it will cause the failure of the study equipment.

The voltage-immunity time curve (V-ITC) consists of two dimensions: the voltage sag amplitude and the immunity time of the sensitive equipment. Different from VTC, V-ITC can record the time when the equipment fails under a certain grid-side voltage amplitude, from when the disturbance affects the equipment to when the equipment is judged to be invalid, such as the time when the ACC suffers a sag to the effective separation of the moving and static contacts. When the ASD suffers from a sag, the time from when the DC link voltage is lower than the undervoltage protection threshold.

Therefore, V-ITC can establish the relationship between grid parameters (the amplitude of the residual voltage at the user's access point or the amplitude of the voltage sag event) and the process parameters (the parameters for judging the equipment or the link where it starts, and the process failure). By studying the V-ITC of each device, the PIT of process link formed by equipment combination can be estimated roughly.

III. METHODOLOGY OF IMMUNITY ASSESSMENT

A. TYPICAL PROCESS STRUCTURE OF ASSEMBLY LINE

For a certain assembly-line process, objects are processed in sequence through steps with specific functions. These steps are the different links in the process, which are functionally compatible with each other but remain independent in their

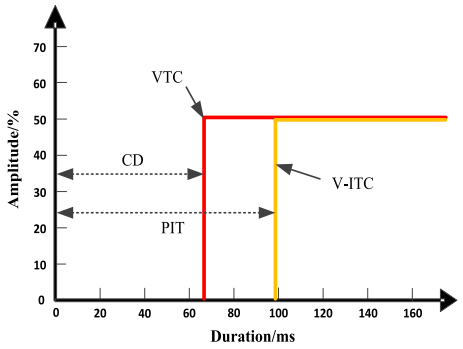

FIGURE 2. Schematic diagram of voltage tolerance curve and voltage-immunity time curve.

response to voltage sag. During a process, the production chain composed of the above items and links is the logistics line. The normal operation of each link requires the maintenance of the corresponding power system. In a certain process link, the power transmission line from the factory power supply to the link power equipment/electrical equipment terminal is the power line. The typical process structure of the assembly line is shown in Fig. 3.

As shown in Fig. 3, the power line can be divided into two parts: the electrical side and the process side. The electrical side refers to the part from power equipment to the power source. On this side, the parameter carrier of disturbance propagation is the electrical quantity, and there are a large number of sensitive equipment (SEQ) such as ACC and ASD. The process side refers to the power equipment (PEQ) such as the electric machine and the load side of the link. On this side, the parameter carrier of disturbance propagation is the process quantity.

In order to improve the response capacity of the production link to the sudden power failure, minimize the loss of equipment and ensure production safety, each process side and link are generally equipped with an interlocking protection system. When the process parameters cross the threshold, the protection will be triggered and the link will fail, thus affecting the whole production line.

B. RESPONSE MECHANISM OF EQUIPMENT FAILURE

Typical voltage sag sensitive devices include PLC, PC, ASD and ACC. At present, most users have adopted UPS devices for protection concerning low-power consumption and relatively key control equipment such as PLC and PC. ACC and ASD have become the sensitive equipment with the greatest influences on users nowadays. As the most commonly used power equipment in the industrial process, the electric machine is worthy of attention on its sag response mechanism and immunity.

1) ACC

When ACC suffers voltage sag, the voltage u at the end of the main coil will drop rapidly, so that the electric current i flowing through the coil decreases. Thus, the magnetic flux in

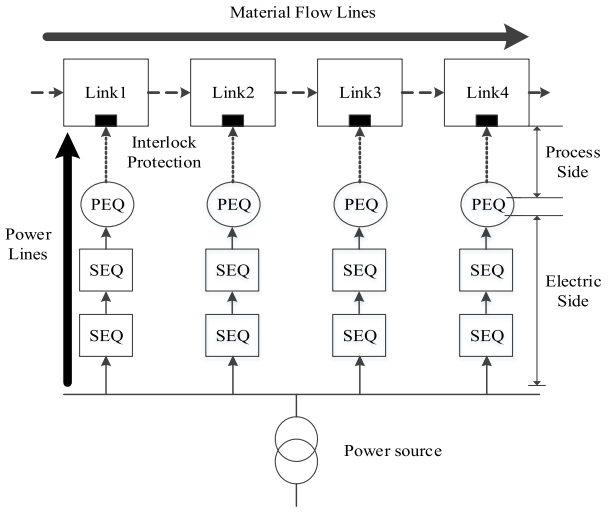

FIGURE 3. Typical assembly line process structure.

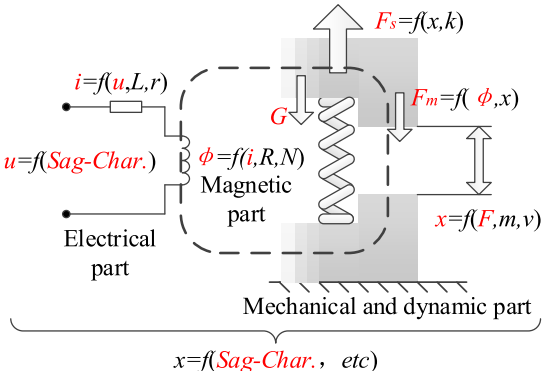

FIGURE 4. Schematic diagram of voltage sag response mechanism of ACC.

the iron core declines, reducing the electromagnetic force so that it is not enough to overcome the effect of spring force. In the end, contact points break away, resulting in power supply interruption of controlled equipment. The voltage sag response mechanism of ACC is shown in Fig. 4. The meaning and impact of G, k, m, v in Fig 4 are shown in the APPENDIX [7].

Based on the response mechanism of ACC, the key parameter to judge its functional failure can be selected as the displacement x, which represents the position of the moving iron core. The threshold value of x is the corresponding displacement value when the contact is effectively separated. When x crosses its threshold, it will lead to power supply interruption. This time can be measured by building an independent indicating loop and using the oscilloscope to monitor potential signals at both ends of ACC. Through plenty of researches, it has been discovered that the action time can be ignored [6], [7]. Therefore, the Δt of ACC approximates 0, namely, PIT approximates CD, which means that the VTC is essentially coincident with V-ITC.

2) ASD

ASD is composed of the rectifier, direct current coupling capacitance and inverter. Among them, the rectifier and

inverter are belonging to the power electronic device with extremely fast response speed, and their output can change according to the variation of input immediately. Thus, the Δt of rectifier and inverter approximates 0, and the Δt of ASD mainly depends on the direct current coupling capacitance.

When ASD suffer sag, it can be concluded from (1) that the output voltage U_{dn} of the rectifier will decrease according to the drop of AC voltage effective value u_n. When the output voltage is lower than the capacitor voltage, the capacitance will discharge through the load side circuit of the inverter. Therefore, the DC bus voltage will experience the transient process described by (2), and eventually reach the steady-state voltage value U_{d-t} after rectification as corresponds to the sag amplitude.

$$U_{dn} = 2.34u_n \tag{1}$$

$$U_{d-t} = U_{d-sag} + (U_{dn} - U_{d-sag})e^{t/RC} \tag{2}$$

where U_{d-sag} is the terminal voltage of ASD when sag occurs. According to this formula, the discharge time of the capacitance mainly depends on the capacitance size C and the resistance value R equivalent to the subsequent load and has nothing to do with the input voltage. Therefore, when the input sag amplitude is lower than a certain threshold V_{th}, leading to the DC voltage after rectification is lower than the DC voltage protection threshold, the time of equipment failure caused by the output of ASD's locking inverter will not change, as shown in Fig. 5. The time from when the sag occurs to when the DC voltage exceeds the threshold is the PIT of ASD. Due to the Δt of the rectifier approximates 0, the CD of ASD equals PIT.

3) MOTOR

Considering the direct-drive motor, when the motor suffers sag, its terminal voltage u drops, and it can be seen from (3) that the electromagnetic torque T_e will decrease. When T_e less than mechanical torque T_m, motor speed n will drop due to the influence of damping torque ΔT_D, at the same time, the motor slip will rise as shown in (6).

$$T_e = \frac{K}{2\pi f}u^2\frac{R'_r/s}{(R'_r/s)^2 + x_k^2} \tag{3}$$

$$\Delta T_D = T_e - T_m \tag{4}$$

$$n = \frac{1}{2\pi}(\frac{\Delta T_D}{J}t_d + \Omega_n) \tag{5}$$

$$s = \frac{n_1 - n}{n_1} \tag{6}$$

where K is the motor structure constant, f is the grid frequency, R'_r is the rotor equivalent resistance, x_k is asynchronous machine short-circuit reactance, s is the slip rate, t_d is the duration of temporary dip, J is moment of inertia, Ω_n is the rated mechanical angular velocity, and n_1 is the synchronous speed of the motor.

In the test and analysis, the threshold value of the motor speed n or slip s is often considered as the critical condition to measure the running state of the equipment. Since the terminal voltage of the direct-fed motor can change abruptly, when the duration is close to the motor PIT, the voltage recovery will cause T_e to return to normal, $\Delta T_D = 0$, by (5) the n will immediately stop further reduced, preventing from triggering the motor protection. Thus CD=PIT.

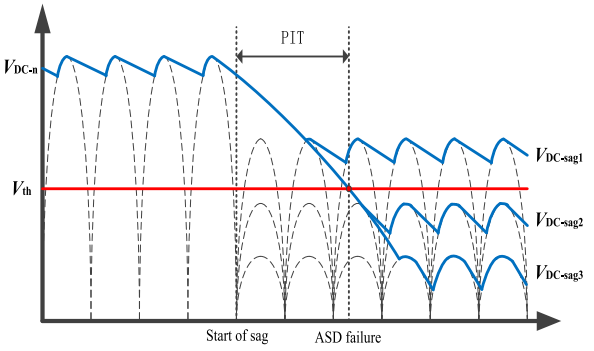

FIGURE 5. Schematic diagram of voltage sag response mechanism of ASD.

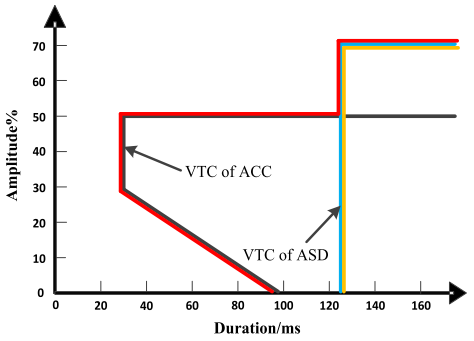

FIGURE 6. Schematic diagram of combined curve comparison diagram of ACC and ASD.

C. IMMUNITY TIME ANALYSIS OF POWER LINE

Considering the typical load conditions, for ACC and ASD, as the DC voltage decay rate of ASD has nothing to do with the input state, when the sag event falls into the VTC envelope of both, the immunity time is consistent with the immunity time of ASD regardless of ACC failure, as shown in Fig. 6. However, the VTC envelope of the two is of great significance, which can be used to judge whether a voltage sag event will lead to the failure of the sensitive equipment in the link and then lead to p.

For the motor used in conjunction with ASD, its output voltage can basically maintain the normal operation of the motor before the ASD is tripped by the voltage sag. When ASD fails, the amplitude of motor terminal voltage is constant to zero, causing the power interruption. Fig.7 provides a diagram showing how a motor is used in conjunction with ASD.

The rated voltage during normal operation of the motor is taken as the reference value for standardization, and the

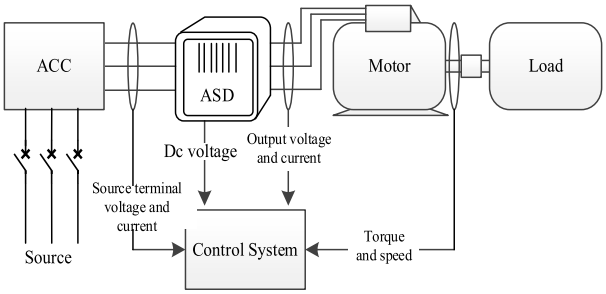

FIGURE 7. The connection diagram of motor and ASD.

relationship between T_e and T_m as shown in (7) [19].

$$T_e = V^2 T_m \tag{7}$$

where V is the temporary voltage drop value after standardization.

Since the slip does not change rapidly in millisecond time relative to the load in the industrial process. Then, the speed change Δn and the final speed can be obtained by considering the initial value as the rated slip.

$$\Delta n = \frac{T_m}{2\pi J} \int_{t_{st}}^{t_{\mathrm{I}}} (V^2(t) - 1)dt \tag{8}$$

$$n_{\mathrm{I}} = n_n + \Delta n \tag{9}$$

where J represents the moment of inertia, t_{st} is the time when temporary drop occurs, t_I and n_I are respectively the time when ASD fails and the rotational speed at the corresponding time, and n_n is the rated rotational speed (r/s).

Furthermore, considering that the amplitude characteristic is constant during the voltage sag, the immune time of the motor can be determined by the following equation.

$$PIT_M = \frac{2\pi J(n_n - n_I)}{T_m(V^2 - 1)} \tag{10}$$

Therefore, the failure of the link can be further judged according to the relationship between the duration of voltage sag and immunity time.

D. THE LINK FAILURE PROBABILITY

The link failure probability can be quantified by equipment failure probability and recovery failure probability. In order to consider the slight difference between the shape factor of VTC and the tolerance of equipment, the general rectangular VTC with fuzzy interval band is usually applied to evaluate the failure probability P_F of equipment [20]. The mathematical model of P_F is shown in (11).

$$P_F = \int_0^{\frac{I-I_0}{I_1-I_0}} f(x)dx \tag{11}$$

where I_o and I_I are the side boundary of the near normal region and the side boundary of the near fault region of the fuzzy interval zone of the equipment VTC curve, respectively, $f(x)$ is the density function of the failure probability of characteristic quantity x in the fuzzy region of the equipment,

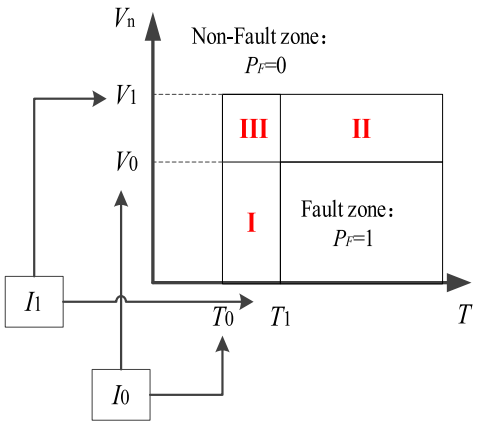

FIGURE 8. The boundary region of the probability of failure.

which can be estimated by data collected through testing and combined with the maximum entropy method [12].

The formula (11) describes the following general structure of VTC. The boundary region of the probability of failure is shown in Fig.8.

When the voltage sag event feature is located in the immune zone, the equipment failure probability $P_F = 0$, and when it is located in the fault zone, $P_F = 1$. I, II, and III in the figure are all uncertain regions, and the failure probability of the equipment in this area depends on the failure probability distribution function of each feature of the equipment. Therefore, a voltage sag event near the outer boundary of the immune zone will cause the probability of equipment failure to be 0, and a voltage sag event near the inner boundary of the fault area will cause the probability of equipment failure to be 1, and the probability of failure is from When the immune zone transitions to the fault zone, it is continuous from 0 to 1.

For the equipment in the same link, all of them are considered as series logical relations due to the high functional compatibility. The failure probability calculation method can adopt the model shown in the following (15). The recovery failure probability is determined by the relationship between immune time and duration of temporary drop. When the immune time is less than the duration of temporary drop, the link will inevitably fail, while when the immune time is not less than the duration of temporary drop, a certain success possibility of recovery exists. This thesis describes this feature from the reverse — recovery failure possibility. Recovery failure rate P_R is related to equipment recovery response time and emergency operation time. Generally, the shorter the temporary sag duration is, the more sufficient the recovery time is and the smaller the recovery failure possibility is.

In order to maintain generality, the normal distribution density function is used to describe the recovery failure possibility under different durations. The mathematical model is as follows

$$f(t) = N(\frac{2t_{st} + PIT}{2}, (\frac{PIT}{6})^2) \tag{12}$$

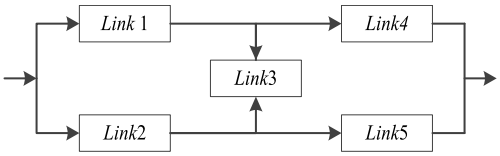

FIGURE 9. Schematic diagram of typical complex stochastic networks.

$$P_R = \int_{t_{st}}^{t_{st}+t_d} f(t)dt \tag{13}$$

where t_{st} is the occurrence time of temporary drop, t_d is the duration of temporary drop, and N is the normal distribution density function. Since the failure of the link needs to meet both equipment failure and process parameter out-of-limit at the same time, the failure probability of the link P_L can be obtained as:

$$P_L = P_F \cdot P_R \tag{14}$$

E. EVALUATION AND ANALYSIS OF LOGISTICS LINE IMMUNITY

The traditional pipeline process can be characterized by simple stochastic networks with only series and parallel relations. If the failure probability P_L of each link is known, the process failure probability P_p can be described in (15).

$$P_{\mathrm{p}} = 1 - \prod_{\mathrm{j}=1}^{\mathrm{k}} (1 - \prod_{\mathrm{i}=1}^{\mathrm{n_j}} P_{\mathrm{Lji}}) \tag{15}$$

where k is the number of parallel link groups, n_j is the number of links in the j_{th} parallel link group, and P_{Lji} is the state of the i_{th} link in the j_{th} parallel link group.

In a large number of pipelined industrial processes, there are multiple parallel production lines. After a link failure in a production line, short-time improvement of work efficiency of the same link in another production line can be applied, transferring the product from the problem production line to the corresponding link of another production line for processing through the transmission device or standby conveying mechanism so as to provide enough time for the recovery of failure link and ensure that the whole production process will not stop. Such a structure needs to be characterized by a complex stochastic network, a typical structure of which is shown in Fig. 9.

Cut set (CS) refers to the combination of links that will cause the process to be interrupted if the combination fails, such as link combination {1, 3, 5}. Minimal cut set (MCS) refers to removing any element from CS, and the cut set is no longer CS.

When all links in the MCS fail, the process will be interrupted. When any link does not fail, the process will not be interrupted. Therefore, MCS method can be used to standardize the network shown in Fig. 9 and use (15) to calculate its failure probability.

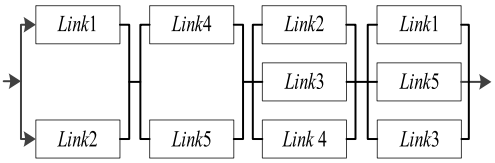

FIGURE 10. Schematic diagram of standardization of complex stochastic networks.

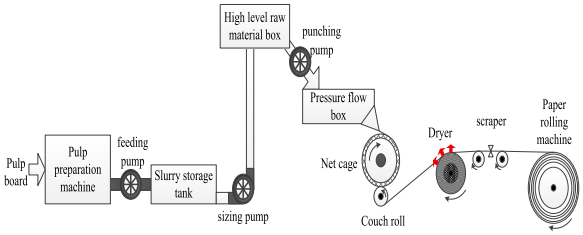

FIGURE 11. Schematic diagram of paper process.

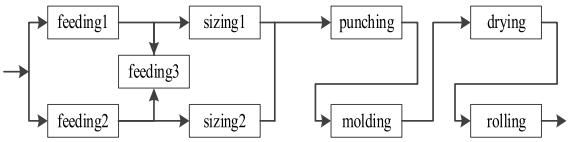

FIGURE 12. Schematic diagram of paper technology logistics line.

IV. CASE

A. PAPER PRODUCTION PROCESS

In this thesis, a paper production process is taken as an example to verify the proposed method. The production process of paper is roughly shown in Fig. 11.

The above processes are roughly divided into the pulp preparation, pulp feeding, drying molding and roll storage. The main power equipment for the pulp preparation is the direct drive motor of the preparation machine and the pulp delivery pump. This production line has two process lines for pulp preparation, and there are two spare pulp pumps in the storage tank between the two processes. When the pressure difference exists on both sides, the pulp pumps in the corresponding direction will be started to pump pulp according to the established flow. This group of pulp pumps can be regarded as a spare link. The main components of the pulp delivery process are pressure flow box and high feeding box, and the key power equipment involved are the sizing pump and the pulp punching pump. The drying molding process includes vacuum mesh cage and dryer parts, and the power equipment involved are the direct drive motor that drives the volt roller and the cylinder body of the dryer to rotate, and the water pump that provides raw material for the steam generator of the dryer. The main power equipment in the roll storage process is the motor that drives the rotation of the reel cylinder. Therefore, the process can be abstractly divided into several links of feeding, sizing, punching, molding, drying and rolling according to the distribution of power equipment, as shown in Fig. 12.

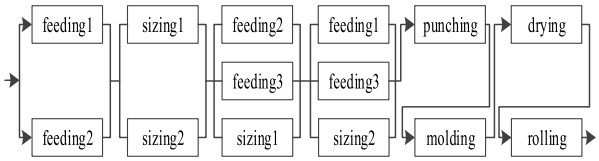

FIGURE 13. Schematic diagram of equivalent logistics line.

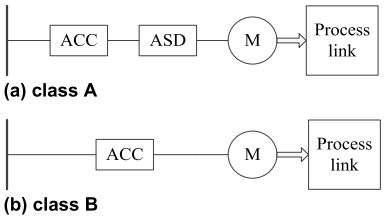

FIGURE 14. Typical power line structures.

TABLE 1. Key parameters of process equipment.

Process equipment	N_{th}(r/s)	N_n(r/s)	T_m(L/s)	J(L/s)
feeding pump	12	24	5	18
sizing pump	12	24	5	18
punching pump	12	24	5	18
Couch roller	10.8	12	15	50
Dryer	3.16	5.4	12	46
Winder	2.53	3.7	10	38

Fig. 12 shows the complex stochastic networks, and the standardized networks can be obtained after MCS processing, as shown in Fig. 13.

Although there are differences in the types of equipment in the power lines of each link, their structures generally fall into the following two categories A and B, as shown in Fig. 14. The sizing pump and the punching pump in this process possess the equivalent power line structures and belong to class A, in which SEQ is ACC and ASD, and PEQ is motor. The power line structures of the paper dryers, winders and couch roller belong to class B, in which SEQ is ACC and PEQ is motor.

The key parameters of process equipment are shown in Table 1. Among them, some key parameters are inconvenient to obtain, substituted by the typical data of the same type of equipment, which will not have a substantial impact on the evaluation method proposed in this thesis.

The boundary value of fuzzy interval of voltage tolerance curve of each equipment used in this example is shown in Table 2. The values in Table 2 are based on the author's investigation of manufacturers with sensitive equipment and the characteristics of the tolerance curve obtained from a large number of tests on sensitive equipment, including the amplitude range and duration range of sensitive equipment.

For three-phase equipment ASD, the following table shows the characteristics of VTC curves under the phasor test conditions of Type I, Type II A and Type III.

TABLE 2. Characteristics of VTC of sensitive equipment.

Sensitive equipment		VTC fuzzy interval boundary value	
		Amplitude range(p.u.) $[V_I, V_{II}]$	Duration range(ms) $[T_I, T_{II}]$
Pulp pump of ACC		[0.5, 0.8]	[60, 100]
Pulp pump of ASD	Type I	[0.4, 0.55]	[20, 100]
	Type II	[0.6, 0.75]	[10, 80]
	Type III	[0.7, 0.8]	[10, 50]

TABLE 3. Statistical event information.

Event	Effective value of amplitude（p.u.）			Duration（ms）
	A	B	C	
1	1.10	1.13	0.96	35
2	0.64	0.62	0.63	628
3	0.98	0.94	0.54	66
4	1.06	0.64	0.62	102
5	1.03	1.05	0.43	500
6	0.92	0.94	0.76	187
7	0.63	0.63	0.65	455
8	0.15	0.15	0.15	564

TABLE 4. Immune time and process failure probability.

process equipment	PIT（ms）	P_L	P_P
feeding pump	127.1	0.548	0.002
sizing pump	127.1	0.548	
punching pump	127.1	0.548	
Couch roll	102.5	0.806	
Dryer	105.4	0.776	
Winder	102.8	0.803	

B. EVALUATION AND ANALYSIS OF IMMUNITY

The statistical data of typical disturbance events of users in one year are shown in Table 3.

The algorithm described in Section III is used to evaluate the process failure probability under various event situations. Taking event 3 as an example, the corresponding results are shown in Table 4.

By making statistics from the aspect of direct loss and indirect loss [12], the maximum loss brought by a long interruption (the most serious case) to the whole production line is recorded as C_{pm}. In this example, the average typical interruption loss value of the mill is 200,000 yuan. According to the survey, the typical loss composition is shown in the Table 5.

Therefore, by combining the loss under the most severe condition with the process failure probability, the economic loss suffered by the enterprise from temporary drop/interruption can be estimated, as described in (16).

$$EL_{\mathrm{py}} = C_{\mathrm{pm}} \sum_{i=1}^{n} P_{\mathrm{P}i} \tag{16}$$

TABLE 5. The information of direct and indirect loss.

Loss type		Loss（Ten thousand yuan）
Direct loss	Waste loss	1
	Capacity loss	16
Indirect loss	Additional loss	3
Total		20

Note: Additional loss include: customer churn, contract breach, labor costs, etc.

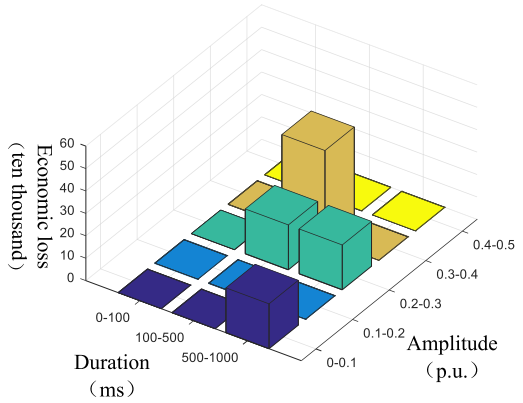

FIGURE 15. Loss distribution of user's three-year sag or short-term interruption.

where EL_{py} is the annual economic loss, n is the number of voltage sag events, and P_{Pi} is the probability of process failure caused by the i_{th} voltage sag event.

The total loss caused by voltage sag events in different sag feature areas to users are visually shown in Fig. 15.

The deeper the sag is, the longer the duration is, the more serious the loss will be. In addition, some events in high frequency feature areas will also bring great losses to users. The evaluation results of the economic loss of users caused by the sag problems in recent one year are shown in Table 6.

It can be seen from Table 6, the difference between the evaluation result of the method proposed in this thesis and the typical loss of the mill is lower than the average loss of 200,000 yuan caused by a short interruption event, indicating that the method proposed in this thesis has a certain effectiveness. Further analysis of the calculation results of the model data built in MATLAB shows that events 1, 3 and 6 have little impact on users, and the corresponding loss assessment results are 0, 0.489 and 0.420 thousand yuan respectively. And the probabilities of failure of sensitive equipment in each link caused by the three events are all less than 0.01. Among them, although the duration of event 6 exceeds the average immune time of each link by 115.35ms and the recovery failure possibility of the link is very high if the equipment fails, the overall failure risk is at a very low level because of the low level of the failure probability of each sensitive equipment to this event, further reflecting the rationality of the model.

TABLE 6. Economic loss of users.

Average loss of single assessment（Ten thousand yuan）	Assess annual loss（Ten thousand yuan）	Research on the loss of typical paper mill users（Ten thousand yuan）
12.51	100.09	113

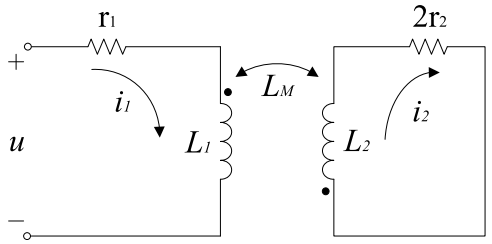

FIGURE 16. Electrical part.

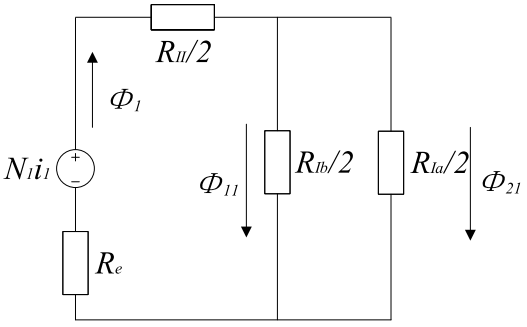

（a） Main coil circuit

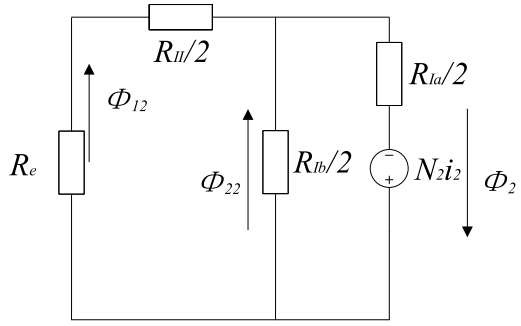

(b) short-circuit loop circuit

FIGURE 17. Main coil and short-circuit loop circuit.

V. CONCLUSION

In this thesis, a method based on traditional VTC, combined with the response mechanism of equipment and process structure, is proposed to evaluate the process immunity. From the electrical disturbance to the change of the process state, it is inevitable to experience the conversion of energy forms such as electric energy to kinetic energy, etc. In this thesis, combining with the characteristics of the process structure of the assembly line, this content is described by the power line and the logistics line. In order to evaluate the process

immune time, V-ITC is introduced based on the analysis of the typical VTC of power line and its response mechanism, and the relationship between the two is described. At the same time, the PIT estimation method of each link in the process is summed up through the study of the response mechanism of power line equipment combination, combined with their respective V-ITC. The estimation of the failure probability of the link is also realized through observing the relationship between PIT, P_F, P_R, and P_L. The process failure probability P_P is further estimated, combined with the logistics topology structure. Besides, the minimum cut set method is used to describe the process stochastic networks more generally, which makes the estimation of process immunity more reasonable.

The proposed method improves the practicability of evaluating the user's voltage sag/interruption disturbance capability, and helps to provide guidance for the user's customized power service in the later stage.

APPENDIX

A. INFLUENCE MECHANISM OF VOLTAGE SAG ON ACC

The mechanism of ACC affected by voltage sag is as follows:

1) Electrical part
The electrical part of ACC is shown in Fig.16. The functional relationship between the main coil inductance voltage and the access point voltage of ACC is as follows:

$$\begin{cases} u = L_1 \dfrac{di_1}{dt} + i_1 r_1 + L_M \dfrac{di_2}{dt} \\ 0 = L_2 \dfrac{di_2}{dt} + 2i_2 r_2 + L_M \dfrac{di_1}{dt} \end{cases} \tag{17}$$

where u is the access point voltage of ACC, i_1 is the main coil current, i_2 is the short-circuit loop current, L_1 and L_2 are the main coil and short-circuit loop inductance, respectively, and L_M is the mutual inductance.

2) Magnetic part
The magnetic part of ACC is shown in Fig.17. Taking the main coil as an example (the relationship in the short-circuit loop is similar), the relationship between the current and the magnetic flux of the iron core is as follows:

$$\phi_1 = \frac{N_1 i_1}{R_e + \frac{R_{II}}{2} + \frac{R_I}{2}} = \frac{N_1 i_1}{R_1} \tag{18}$$

$$\phi_{11} = \phi_1 \frac{R_{Ia}}{R_{Ia} + R_{Ib}} = \frac{N_1 i_1}{R_{11}} \tag{19}$$

$$\phi_{21} = \phi_1 \frac{R_{Ib}}{R_{Ib} + R_{Ia}} = \frac{N_1 i_1}{R_{21}} \tag{20}$$

where Φ is the magnetic flux of each magnetic circuit branch, R is the magnetic resistance of each magnetic circuit branch, and N is the number of turns of each coil.

3) Mechanical and dynamic part
The relationship between electromagnetic force and magnetic flux is as follows:

$$F_{mag} = \frac{(\phi_1 + \phi_{12})^2}{2\mu_0 S_e} + \frac{(\phi_2 + \phi_{21})^2}{2\mu_0 \cdot 2S_{Ia}} + \frac{(\phi_{11} - \phi_{22})^2}{2\mu_0 \cdot 2S_{Ib}} \tag{21}$$

where μ_0 is the air permeability, and S is the area of the magnetic surface of each iron core.
The spring force formula is as follows:

$$F_s = nkx \tag{22}$$

where n is the number of springs, k is the spring stiffness coefficient, and x is the displacement of the moving iron core.
The moving iron core displacement formula is as follows:

$$\frac{d^2x}{d^2t} = \frac{1}{m}(F_s - mg - F_{\text{mag}}) \tag{23}$$

$$\frac{dx}{dt} = v_0 \Delta t + \frac{1}{2} a_0 \Delta t^2 \tag{24}$$

where m is the mass of the moving iron core, g is the gravitational constant, gravity G is mg, and x is the displacement.

B. THE IMPACT OF G, k, m, v

1) When G and F_{mag} are larger, the moving iron core needs to overcome the greater reaction force to do work to move up, and the ACC is not easy to trip at this time.
2) When k increases, F_s is larger, and the power for the iron core to move up increases, and ACC is easier to trip.
3) When the moving iron core speed v is large, the operating state of the iron core is more difficult to change. Generally, when the speed exceeds a certain threshold, the displacement x will inevitably be exceeded, resulting in effective separation of the moving and static contacts and ACC tripping.
4) The impact of the sag on ACC is reflected in the impact on F_{mag}, which is ultimately affected by the terminal voltage u, and the two are in a positive correlation. The sag makes u decrease and F_{mag} decreases, so that the displacement x exceeds the limit.

REFERENCES

[1] J. Yhee Chan, J. V. Milanović, and A. Delahunty, "Risk-based assessment of financial losses due to voltage sag," *IEEE Trans. Power Del.*, vol. 26, no. 2, pp. 492–500, Apr. 2011.
[2] S. Jothibasu and M. K. Mishra, "An improved direct AC–AC converter for voltage sag mitigation," *IEEE Trans. Ind. Electron.*, vol. 62, no. 1, pp. 21–29, Jan. 2015.
[3] Y. Han, Y. Feng, P. Yang, L. Xu, Y. Xu, and F. Blaabjerg, "Cause, classification of voltage sag, and voltage sag emulators and applications: A comprehensive overview," *IEEE Access*, vol. 8, pp. 1922–1934, 2020.
[4] A. K. Goswami, C. P. Gupta, and G. K. Singh, "Voltage sag assessment in a large chemical industry," *IEEE Trans. Ind. Appl.*, vol. 48, no. 5, pp. 1739–1746, Sep. 2012.

[5] N. Ashraf, T. Izhar, G. Abbas, A. B. Awan, U. Farooq, and V. E. Balas, "A new single-phase AC voltage converter with voltage buck characteristics for grid voltage compensation," *IEEE Access*, vol. 8, pp. 48886–48903, 2020.
[6] S. Z. Djokic, J. V. Milanovic, and D. S. Kirschen, "Sensitivity of AC coil contactors to voltage sags, short interruptions, and undervoltage transients," *IEEE Trans. Power Del.*, vol. 19, no. 3, pp. 1299–1307, Jul. 2004.
[7] X. Xiao, H. He, and Y. Wang, "Analytical model of AC contactors for studying response mechanism to multi-dimensional voltage sag characteristics and its novel applications," *IET Gener., Transmiss. Distrib.*, vol. 13, no. 17, pp. 3910–3920, Sep. 2019.
[8] A. Honrubia-Escribano, E. Gómez-Lázaro, A. Molina-Garcia, and S. Martín-Martínez, "Load influence on the response of AC-contactors under power quality disturbances," *Int. J. Electr. Power Energy Syst.*, vol. 63, pp. 846–854, Dec. 2014.
[9] S. Z. Djokic, K. Stockman, J. V. Milanovic, J. J. M. Desmet, and R. Belmans, "Sensitivity of AC adjustable speed drives to voltage sags and short interruptions," *IEEE Trans. Power Del.*, vol. 20, no. 1, pp. 494–505, Jan. 2005.
[10] S. Z. Djokic, J. Desmet, G. Vanalme, J. V. Milanovic, and K. Stockman, "Sensitivity of personal computers to voltage sags and short interruptions," *IEEE Trans. Power Del.*, vol. 20, no. 1, pp. 375–383, Jan. 2005.
[11] H. He, X. Xiao, C. Li, and H. Zhang, "Fuzzy reasoning model for risk assessment of voltage sag loss for sensitive users," *Proc. CSEE*, vol. 40, no. 20, pp. 6527–6536, Oct. 2020.
[12] C. Li, H. Li, and B. Liu, "Risk assessment based on process immunity uncertainty for industrial customers' financial losses due to voltage sags," *Electr. Power Autom. Equip.*, vol. 36, no. 12, pp. 136–142, Dec. 2016.
[13] *Voltage Dip Immunity of Equipment and Installations*, CIGRE, Paris, France 2010.
[14] J. C. Cebrian, J. V. Milanović, and N. Kagan, "Probabilistic assessment of financial losses in distribution network due to fault-induced process interruptions considering process immunity time," *IEEE Trans. Power Del.*, vol. 30, no. 3, pp. 1478–1486, Jun. 2015.
[15] J. C. Cebrian, N. Kagan, and J. V. Milanović, "Probabilistic estimation of distribution network performance with respect to voltage sags and interruptions considering network protection setting—Part I: The methodology," *IEEE Trans. Power Del.*, vol. 33, no. 1, pp. 42–51, Feb. 2018.
[16] J. C. Cebrian, N. Kagan, and J. V. Milanović, "Probabilistic estimation of distribution network performance with respect to voltage sags and interruptions considering network protection Setting—Part II: Economic assessment," *IEEE Trans. Power Del.*, vol. 33, no. 1, pp. 52–61, Feb. 2018.
[17] L. E. Weldemariam, H. J. Gärtner, V. Cuk, J. F. G. Cobben, and W. L. Kling, "Experimental investigation on the sensitivity of an industrial process to voltage dips," in *Proc. IEEE Eindhoven PowerTech*, Eindhoven, The Netherlands, Jun. 2015, pp. 1–6.
[18] H.-Y. He, W.-H. Zhang, Y. Wang, and X.-Y. Xiao, "A sensitive industrial process model for financial losses assessment due to voltage sag and short interruptions," *IEEE Trans. Power Del.*, early access, Jun. 30, 2020, doi: 10.1109/TPWRD.2020.3006017.
[19] M. H. J. Bollen, *Understanding Power Quality Problem: Voltage Sag and Interruption*. Piscataway, NJ, USA: IEEE, 2000.
[20] J. V. Milanovic and C. P. Gupta, "Probabilistic assessment of financial losses due to interruptions and voltage sags—Part I: The methodology," *IEEE Trans. Power Del.*, vol. 21, no. 2, pp. 918–924, Apr. 2006.

ANJUNGUO HUANG is currently pursuing the degree with Sichuan University, China. His research interests include power quality assessment and analysis.

XIANYONG XIAO (Senior Member, IEEE) received the Ph.D. degree from Sichuan University, China, in 2010. He is currently a Professor with the College of Electrical Engineering, Sichuan University. His research interests include power quality and its control, distribution systems reliability, and smart grid.

YING WANG (Senior Member, IEEE) received the B.S., M.S., and Ph.D. degrees from Sichuan University, China, in 2004, 2007, and 2014, respectively. She is currently a Professor with Sichuan University. Her research interest includes the area of assessing the behavior of sensitive equipment during voltage sags.